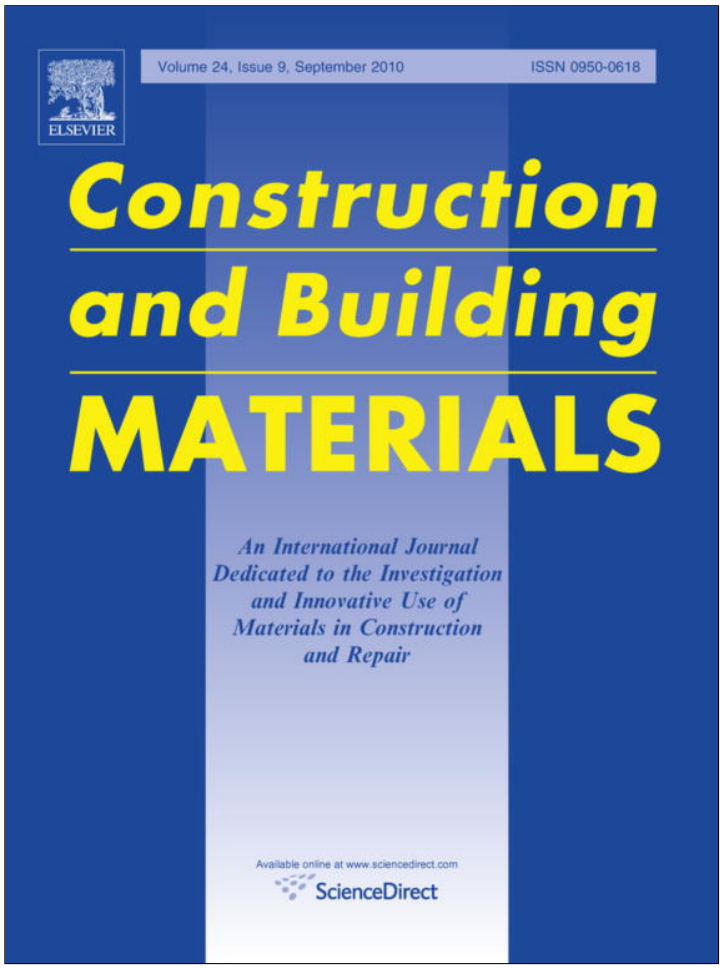

Construction and Building Materials 24 (2010) 1690–1699

Contents lists available at ScienceDirect

Construction and Building Materials

journal homepage: www.elsevier.com/locate/conbuildmat

Compressive strength of circular hollow reinforced concrete confined by an internal steel tube

Taek Hee Han [a], Ki Yong Yoon [b], Young Jong Kang [c,*]

[a] R&D Center, Seoul Metro, Seoul 137-060, Republic of Korea
[b] Department of Civil Engineering, Sunmoon University, Asan, Chungnam 336-708, Republic of Korea
[c] Department of Architectural, Civil and Environmental Engineering, Korea University, Seoul 136-713, Republic of Korea

ARTICLE INFO

Article history:
Received 29 September 2008
Accepted 9 February 2010
Available online 15 March 2010

Keywords:
Concrete
Confinement
Strength
Composite
Hollow

ABSTRACT

When concrete is confined, its strength is enhanced by confining stress. Therefore many researchers have studied the confinement and its effect in a reinforced concrete (RC) member. However, their research has focused on making confining pressure from the outside of the member. In a hollow RC member, it is impossible to confine its concrete triaxially because it has a hollow section. The concrete in a hollow RC member is usually in the state of biaxially confinement, and it shows lower strength than the concrete in a solid RC member, which is confined triaxially. In this study, the compressive strength of the concrete in a hollow RC column with an internal steel tube was investigated. The internal tube makes the concrete confined triaxially with internal confinement. To show the existence and the effect of the internal confinement, an experiment was performed. Fourteen specimens were tested. The test results showed that the internal confinement existed and made the concrete in the state of triaxial confinement.

1. Introduction

Confined concrete shows much larger strength and ductility than unconfined concrete. Fig. 1 shows the difference of stress–strain relations between confined and unconfined concrete. The enhanced strength and ductility of confined concrete depend on the confining pressure. Therefore many researchers have studied how to effectively confine concrete. For a reinforced concrete (RC) column, Roy and Sozen [1] tested rectangular concrete members confined by transverse reinforcements. They presented that there was no increase in concrete strength, but a significant increase in ductility could be achieved. Iyengar et al. [2] and Desayi et al. [3] showed that there was a significant increase in both strength and ductility of concrete members including circular steel spirals. Vallenas et al. [4], Sheikh and Uzumeri [5], and Scott et al. [6] tested more realistically scaled specimens of real building columns. They presented the stress–strain relations of the specimens. The test results for confined square sections with rectangular and octagonal shaped transverse reinforcements indicated that the strength and the ductility of the specimens were significantly enhanced. Recently, many researchers ([7–10]) made analytical models for the explanation of the effect of concrete confinement. The analytical results showed widely divergent opinions about the increase in strength and ductility of concrete as the shape of its confined section. Mander et al. [11] suggested a unified concrete model to define the stress–strain relations for square and circular sections. It is widely used to explain the effect of concrete confinement. Many other researchers have also studied the concrete confined by composite material. Lin et al. [12,13] performed numerical and experimental studies for the compressive concrete strength confined by composite material. Binici [14] suggested an analytical model for fiber reinforced polymer (FRP) and steel confined concrete. Mirmiran et al. [15] and Saafi et al. [16] studied concrete columns confined by FRP.

But all of these studies focused on confining the outside of a concrete member. They are effective in confining a solid RC member triaxially, however, they are not so effective in confining a hollow RC member, because it has a hollow section and its concrete is confined biaxially. Therefore, to confine the concrete in a hollow RC member triaxially, it is necessary to confine the concrete of the inner face of the column. To make the concrete of a hollow RC member under triaxial confinement, an internally confined hollow (ICH) RC column was introduced, and its nonlinear concrete model was proposed by Han et al. [17]. Their concrete model is based on the unified concrete model proposed by Mander et al. [11]. An ICH RC column is a hollow RC column having a flat or corrugated tube inside of itself to confine the concrete internally. Fig. 2 shows the cross section of an ICH RC column. In this study, to prove the existence of the internal confinement, an experiment was performed. Fourteen real-sized and partial specimens were tested, and the effect of internal confinement was investigated.

* Corresponding author. Tel.: +82 2 3290 3317; fax: +82 2 921 5166.
E-mail address: yjkang@korea.ac.kr (Y.J. Kang).

0950-0618/$ - see front matter © 2010 Elsevier Ltd. All rights reserved.
doi:10.1016/j.conbuildmat.2010.02.022

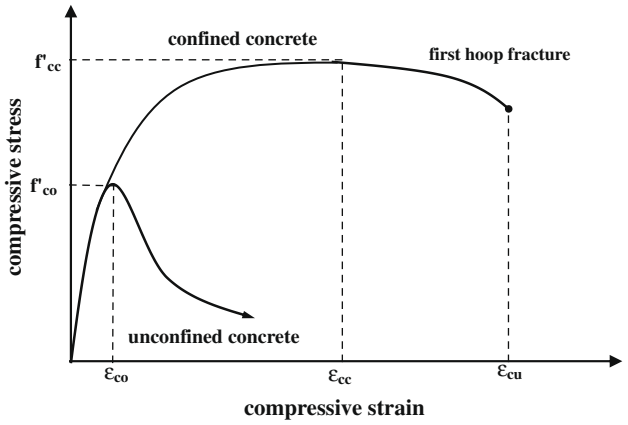

Fig. 1. Stress–strain relations of confined and unconfined concrete.

2. Basic concept of ICH RC column

Fig. 3 shows the biaxially confined state of the concrete in a hollow RC column when an axial load is applied on the concrete until its transverse reinforcement yields. Fig. 3a shows the cross section of a hollow RC column. Fig. 3b shows its free body diagram when it is axially loaded. Where d is the diameter of a confined concrete wall, t is the thickness of the confined concrete wall, f_y is the yield stress of the transverse reinforcement, and A_b is the cross sectional area of the transverse reinforcement. When a hollow RC column is axially loaded, transverse reinforcements make passive confining pressure (f_r) by Poisson's effect. The concrete wall element is compressed in the circumferential direction by arching action. However, the concrete wall element is not confined in the radial direction because nothing can make confining pressure at the internal surface of the concrete wall element. In this state, the concrete wall element is biaxially confined by the axial stress (f_1) and the circumferential stress (f_2). Therefore, a brittle failure may occur on the concrete wall element.

Fig. 4 shows the triaxially confined state of the concrete by inner and outer transverse reinforcements in a hollow RC column. Fig. 4a shows its cross section and Fig. 4b shows its free body diagram when it is axially loaded. When the column is axially loaded, the outer transverse reinforcements make passive confining pressure by Poisson's effect. And its concrete wall element is compressed in the circumferential direction by an arching action. The inner transverse reinforcements make passive confining pressure which is defined by internal confinement to the wall element. Therefore, the concrete wall element is triaxially confined by f_1, f_2 and the passive confining pressure (f_3) in the radial direction as shown in Fig. 4b and c. But in this case, the internal transverse reinforcements can easily buckle after the spalling of the inner cover concrete. After the buckling, the concrete wall is under biaxial confinement. Therefore, a brittle failure may occur after the buckling of the inner transverse reinforcement. The inner transverse reinforcements cannot offer continuous confinement because they are not located continuously.

To solve this problem, an ICH RC column was suggested by Han et al. [17]. In the ICH RC column, a tube is placed at the inner face of the column, as shown in Fig. 5, to confine the concrete wall element. In this column, continuous confining stress is offered by the internal tube, and it confines the concrete wall element triaxially. This confining effect enhances the strength of the concrete. An ICH RC column was developed with this concept of internal confinement. The behavior of an ICH RC column has been studied by Han et al. [17], and they suggested a nonlinear concrete model for an ICH RC column. In this study, an experiment was performed to show the existence and the effect of internal confinement by an internal tube in an ICH RC column. Fourteen specimens were

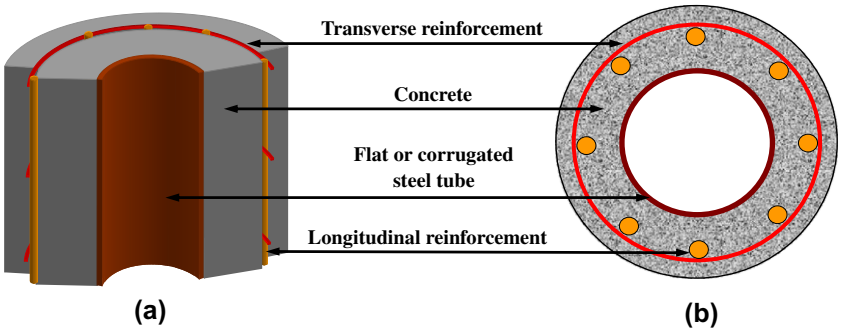

Fig. 2. Cross section of a circular ICH RC column.

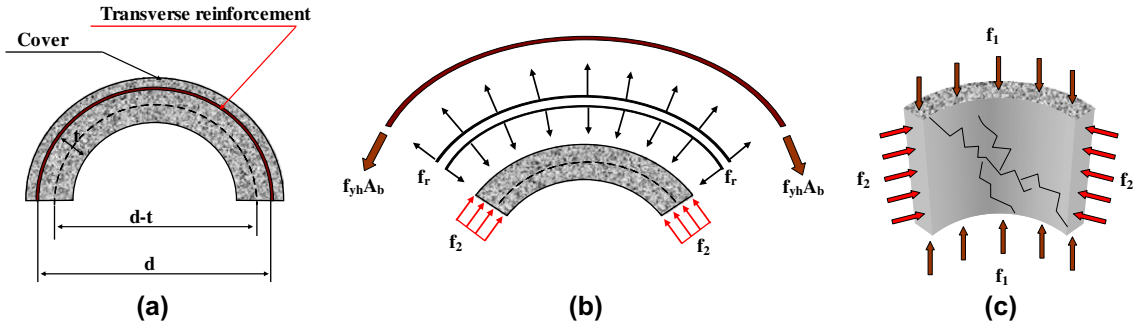

Fig. 3. Hollow RC column without internal hoop reinforcement (biaxially confined).

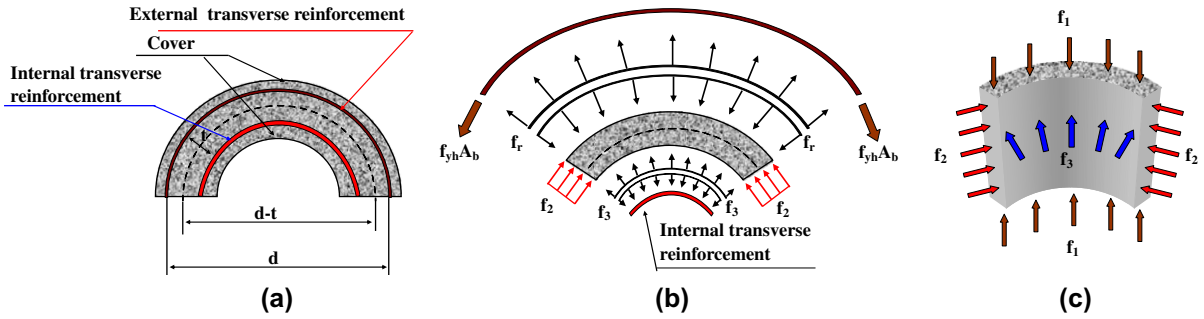

Fig. 4. Hollow RC column with internal hoop reinforcement (triaxially confined).

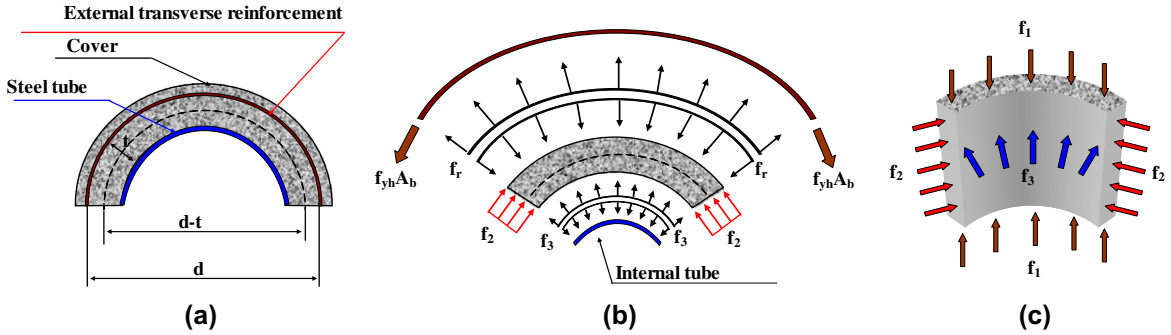

Fig. 5. Triaxially confined state of concrete in ICH RC column by an internal tube.

tested to show the enhanced strength of concrete by internal confinement.

3. Failure modes of ICH RC column

3.1. Uniaxial stress–strain model of concrete

Mander et al. [11] proposed a unified stress–strain approach to predict the pre-yield and post-yield behavior of confined concrete members subjected to axial compressive stress. They adopted utilized Eq. (1) proposed by Popovics [18] to develop the unified stress–strain relation of the confined concrete. This model is based on constant confining pressure.

$$f_c = \frac{f'_{cc}x \cdot r}{r - 1 + x^r} \tag{1}$$

where $x = \frac{\varepsilon}{\varepsilon_{cc}}$, $r = \frac{E_c}{(E_c - E_{sec})}$, $E_{sec} = \frac{f'_{cc}}{\varepsilon_{cc}}$, f_c = concrete stress, f'_{cc} = confined strength of concrete, ε = uniaxial strain, ε_{cc} = strain at peak concrete strength, and E_c = tangent modulus of unconfined concrete.

The peak concrete strength for confined concrete (f'_{cc}) and the strain at peak concrete strength are calculated with Eqs. (2) and (3). The strain at peak concrete strength (ε_{cc}) is given as a function of the strain at peak strength of unconfined concrete (ε_{co}). The value of ε_{co} is usually regarded as 0.002.

$$f'_{cc} = f'_c\left(2.254\sqrt{1 + \frac{7.94f'_l}{f'_c}} - \frac{2f'_l}{f'_c} - 1.254\right) \tag{2}$$

$$\varepsilon_{cc} = \varepsilon_{co}\left[1 + 5\left(\frac{f'_{cc}}{f'_c} - 1\right)\right] \tag{3}$$

where f'_c = strength of unconfined concrete, f'_l = effective constant lateral confining pressure.

In a RC column, transverse reinforcements cannot confine the entire core concrete because of the spacing between transverse reinforcements. Therefore, the effective constant confining pressure has to be used instead of the constant confining pressure (f_l). The effective constant confining pressure can be calculated by Eq. (4) using the reduction coefficient (k_e).

$$f'_l = k_e \cdot f_l \tag{4}$$

3.2. Equilibrium in a hollow RC column

Fig. 6 shows the half section of a hollow RC column when axial load acts on it. The transverse reinforcement does not exert any lateral pressure on the concrete core in the radial direction because the hollow region does not have any confinement. There is only circumferential pressure on the concrete by arching action. The confining stress in the circumferential direction (f_{lc}) can be calculated with Eq. (5) and the confining stress in the radial direction (f_{lr}) is assumed zero. From the assumption of $f_{lr} = 0$ and $f_{lc} \neq 0$, the concrete in a hollow RC column is considered to be biaxially confined. The effective lateral pressure (f_l') at the yield of a transverse reinforcement is defined as the average of radial and circumferential confining stress components as Eq. (6). When concrete is confined by hoops or spirals, the reduction coefficient (k_e) is 0.95 ([11]).

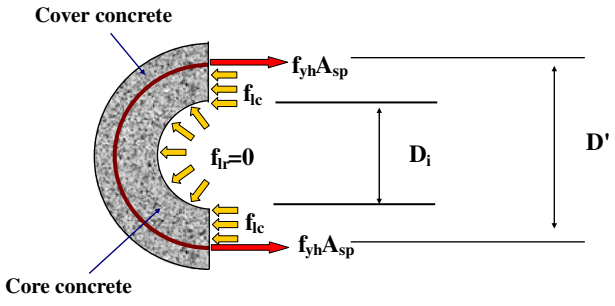

Fig. 6. Confining stress on concrete in a hollow RC column.

$$f_{lc} = \frac{2f_{yh}A_{sp}}{(D' - D_i)s} \tag{5}$$

$$f'_l = 0.5(f'_{lr} + f'_{lc}) \tag{6}$$

where D' = diameter of confined core concrete, D_i = diameter of hollow section, f_{yh} = yield strength of a transverse reinforcement, A_{sp} = cross sectional area of a transverse reinforcement, s = spacing of adjacent two transverse reinforcements, f'_{lr} = effective confining stress in the radial direction, f'_{lc} = effective confining stress in the circumferential direction.

Mander et al. [11] researched the multiaxial strength criterion when concrete is confined by different confining pressures along each direction. Based on the results of experimental study, a chart was suggested according to the ratio of the confining stress and confined strength. It includes graphs for the cases of biaxial and triaxial confining condition. By regression for the curve of biaxial condition in the chart, the confined strength of concrete in a hollow RC column can be proposed as Eq. (7).

$$f'_{cc} = -2.75\frac{f'^2_{lc}}{f'_c} + 1.835f'_{lc} + f'_c \tag{7}$$

3.3. Equilibrium in an ICH RC column

Han et al. [17] defined failure modes of an ICH RC column. Fig. 7 shows the half section of an ICH RC column when axial load acts on the concrete only. Considering the failures of the internal tube and the transverse reinforcement, three failure modes can be defined as Eq. (8). In the first failure mode, the internal tube fails by buckling or yielding before the transverse reinforcement yields. The reverse condition is the second failure mode. In the third failure mode, the internal tube and transverse reinforcement fail simultaneously.

$$f_{tube} > f_{\lim} = \text{smaller}(f_{yt}, f_{bk}): \text{ failure mode 1} \tag{8a}$$

$$f_{tube} < f_{\lim} = \text{smaller}(f_{yt}, f_{bk}): \text{ failure mode 2} \tag{8b}$$

$$f_{tube} = f_{\lim} = \text{smaller}(f_{yt}, f_{bk}): \text{ failure mode 3} \tag{8c}$$

where f_{tube} = stress acting on the internal tube in the radial direction (i.e. lateral pressure), f_{yt} = yield strength of the internal tube, f_{bk} = buckling strength of the internal tube, and $f_{\lim}$ = smaller value between yield strength and buckling strength of the internal tube.

In the first failure mode, the concrete in the column is completely confined before the internal tube fails. After the internal tube fails, it is assumed to exert no more passive confining pressure. Therefore, after the internal tube fails, the concrete is under the biaxial confinement. In the second failure mode, the concrete is completely confined until the whole column fails by the yielding of the transverse reinforcement. The failure of the whole column depends on the yielding of the transverse reinforcement. Because the triaxial confinement is completely maintained until the failure of the transverse reinforcement, the concrete in the column has equal strength to that in a solid RC column in this case. The confining pressure in the circumferential direction is equal to that in the radial direction ($f_{lc} = f_{lr}$). The third failure mode is a very rare case, and it has a similar failure pattern to the second failure mode. Considering 'failure mode 2' and 'failure mode 3', Eqs. (9) and (10) can be derived from Fig. 7a and b. By substituting Eq. (10) to Eq. (9), the confining pressure acting on the concrete is given as Eq. (11), where t is the thickness of the internal tube.

$$\{f_l(D' - D_i) + 2f_{tube}t\}s = 2f_{yh}A_{sp} \tag{9}$$

$$f_{tube} = \frac{f_l D_i}{2t} \tag{10}$$

$$f_l = \frac{2f_{yh}A_{sp}}{D's} \tag{11}$$

3.4. Yielding condition of internal tube

The yielding of an internal tube before the transverse reinforcement yields can be guaranteed by controlling the thickness of the internal tube. Eq. (12) is derived from Eqs. (10) and (11). To avoid the premature failure of the column, f_{tube} must be less than f_{yt}. The minimal thickness of the internal tube to prevent its premature yielding failure (t_{yt}) is calculated by Eq. (13).

$$f_{tube} = \frac{D_i \cdot f_{yh} \cdot A_{sp}}{D' \cdot s \cdot t} < f_{yt} \tag{12}$$

$$t_{yt} = \frac{D_i \cdot f_{yh} \cdot A_{sp}}{D' \cdot s \cdot f_{yt}} \tag{13}$$

3.5. Buckling condition of internal tube

The internal tube of an ICH RC column is unilaterally restrained by concrete. Because of this unilateral boundary condition, the internal tube has a different buckling strength from that of an arch or ring with bilateral conditions. The buckling strength of unilaterally restrained arches has been studied by many researchers. Kerr and Soifer [19] proposed the buckling strength of a circular arch by linearization of the prebuckling deformation. Haftka et al. [20] suggested the bifurcation buckling strength and snap-through buckling strength of a circular shallow arch using the Koiter's method. Sun and Natori [21] proposed the numerical solution of a large deformation problem by considering the unilateral boundary condition. Table 1 presents the buckling load coefficients for a circular arch suggested by previous researchers.

In this study, the buckling behavior of the internal tube is considered as the snap-through behavior of a circular shallow arch because the internal tube can only buckle inward. The buckling coefficient proposed by Kerr and Soifer [19] was adopted to estimate the buckling strength of the internal tube. From their study, the buckling strength of a circular shallow arch (p_0) can be

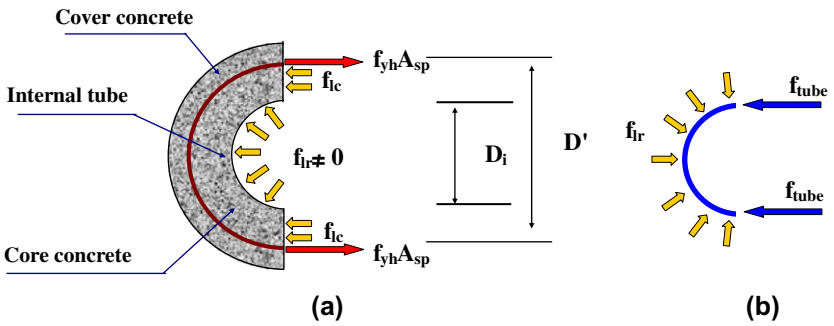

Fig. 7. Confining stress on concrete in an ICH RC column.

Table 1
Circular arch buckling load coefficients.

Case	Buckling load coefficient		
	Kerr and Soifer [19]	Haftka et al. [20]	Sun and Natori [21]
Bifurcation	1.91	1.86	1.90
Snap-through	2.27	2.17	2.28

calculated with Eq. (14). By substituting the snap-through buckling coefficient (2.27) for the normalized nondimensional pressure ($\bar{p}$) in Eq. (14), the buckling strength of the internal tube (f_{bk}) can be calculated by Eq. (15).

$$p_0 = \bar{p}\frac{EI}{R^2 t} \tag{14}$$

$$f_{bk} = 2.27\frac{EI}{R^2 t} = \frac{2.27}{3}\frac{t^2 E}{D_i^2} \tag{15}$$

where E = modulus of elasticity, I = moment of inertia, R = radius of the internal tube.

Table 2
Planned specimens.

Specimen	D (mm)	D' (mm)	D_i (mm)	D/D_i	t (mm)
D150H65T0	1500	1400	975	0.65	–
D150H65T6	1500	1400	975	0.65	6
D150H75T0	1500	1400	1125	0.75	–
D150H75T2	1500	1400	1125	0.75	2
D150H75T6	1500	1400	1125	0.75	6
D200H65T2	2000	1900	1300	0.65	2
D200H65T4	2000	1900	1300	0.65	4
D200H65T6	2000	1900	1300	0.65	6
D200H70T0	2000	1900	1400	0.70	–
D200H70T4	2000	1900	1400	0.70	4
D200H70T6	2000	1900	1400	0.70	6
D200H75T0	2000	1900	1500	0.75	–
D200H75T2	2000	1900	1500	0.75	2
D200H75T6	2000	1900	1500	0.75	6

Table 3
Designed reinforcement.

Diameter of specimen (mm)	Longitudinal reinforcement		Transverse reinforcement		
	Diameter (mm)	Total nominal area (mm^2)	Diameter (mm)	Spacing (mm)	Reinforcement ratio
1500	29	642.4	19	110	0.0075
2000	32	794.2	22	110	0.0075

To prevent the premature buckling failure of the internal tube before the yielding of the transverse reinforcement, the buckling strength of the internal tube must be larger than the confining pressure acting on the concrete when the transverse reinforcement yields. With this design concept and Eq. (15), a failure criterion can be defined as Eq. (16). From Eq. (16), the required minimal thickness of the internal tube to prevent its premature buckling failure (t_{bk}) can be calculated by Eq. (17).

$$f_{bk} = \frac{2.27}{3}\frac{t^2 E}{D_i^2} > f_l = \frac{2 f_{yh} A_{sp}}{D's} \tag{16}$$

$$t_{bk} = \sqrt{\frac{6}{2.27}\frac{D_i^2 f_{yh} A_{sp}}{D'sE}} \tag{17}$$

The required minimal thickness of the internal tube to prevent its premature failure ($t_{\lim}$) can be defined as the larger value between t_{yt} and t_{bk} from Eqs. (13) and (17), respectively. When an ICH RC column fails as the 'failure mode 1', this failure mode can be classified into two failure modes. One is a failure by the yield of the internal tube. The other is a failure by buckling of the internal tube. These failure modes can be determined by the comparison of the yield strength (f_{yt}) and the buckling strength (f_{bk}) of the internal tube. It is also possible to determine the failure mode with respect to the comparison of the thickness of an internal tube (t) and its required minimal thickness for yield (t_{yt}) and buckling (t_{bk}).

4. Experimental program

4.1. Specimens

Fourteen fan-shaped ICH RC specimens were tested to verify the existence and the effect of internal confinement by the internal tube. The specimens were designed to have large diameters as a real column to minimize any size effect that would happen by reducing their sizes. Their outer diameters (D) were 1500 mm and 2000 mm. If a fan-shaped specimen had a small angle, the arching action to make circumferential confining pressure would not be exerted. Therefore, all specimens were designed to have enough angles to exert circumferential confining pressure by the results of finite element analyses [23]. The main experimental parameter was the failure mode of the specimen. To conduct planned failure modes, specimens were designed to have the confined diameters of 1400 mm and 1900 mm, the hollow ratios (D_i/D) of 0.65, 0.70, and 0.75. The internal tubes were designed to have the thicknesses (t) of 0 mm, 2 mm, 4 mm, and 6 mm. In the three types of the designed specimens, the first type was the specimen to represent a hollow RC column having no internal steel tube (i.e. $t = 0$). The second type was the specimen to represent an ICH RC column having the 'failure mode 1', which would have premature failure of the internal tube. The last type was the specimen to represent an ICH RC column having the 'failure mode 2', which would have a yield failure of a transverse reinforcement. For the comparison of the test results, all specimens were designed to have equal confining pressures by having equal transverse reinforcement ratios. Table 2 shows the planned specimens and their parameters.

In designing the specimens, the longitudinal reinforcement ratio was determined as 1%. It results from the guidance in 'Korea Specification of Highway Bridges (KSHB)' [22]. The transverse reinforced ratio was also determined considering the

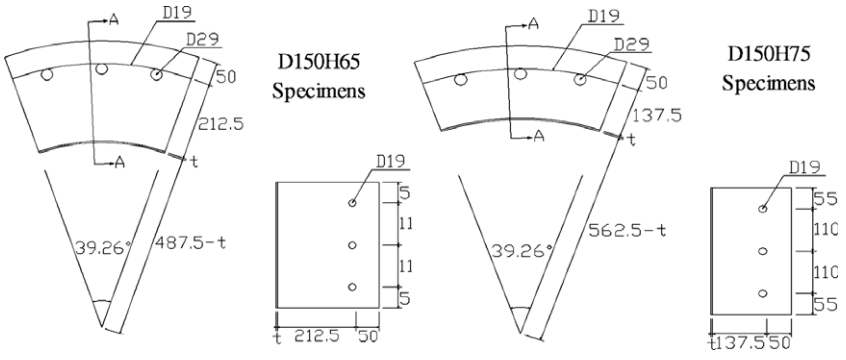

Fig. 8. Designed specimens of D150 Series (mm).

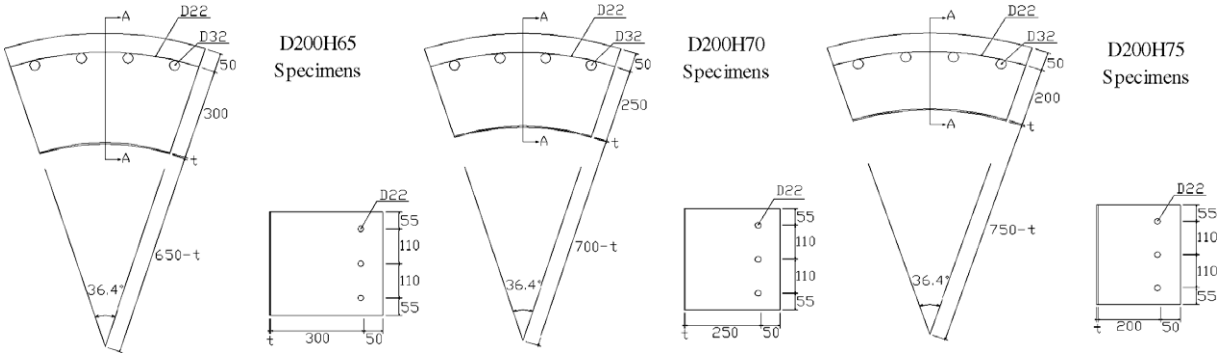

Fig. 9. Designed specimens of D200 Series (mm).

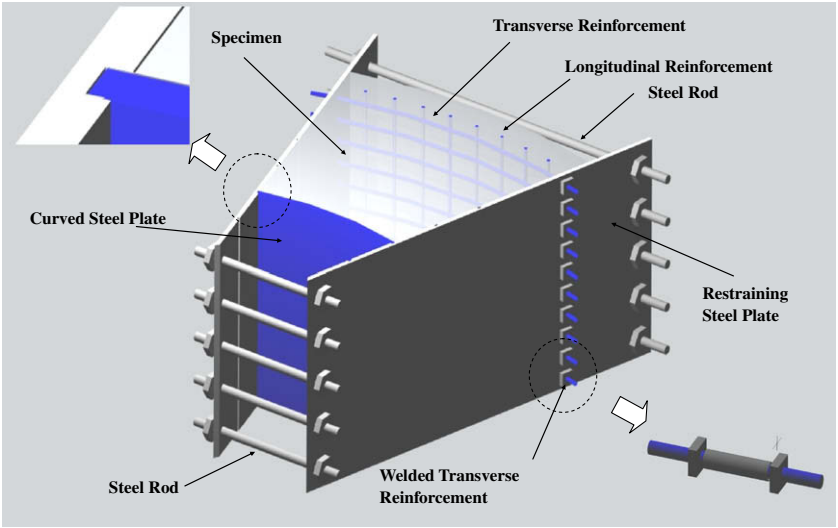

Fig. 10. Test device.

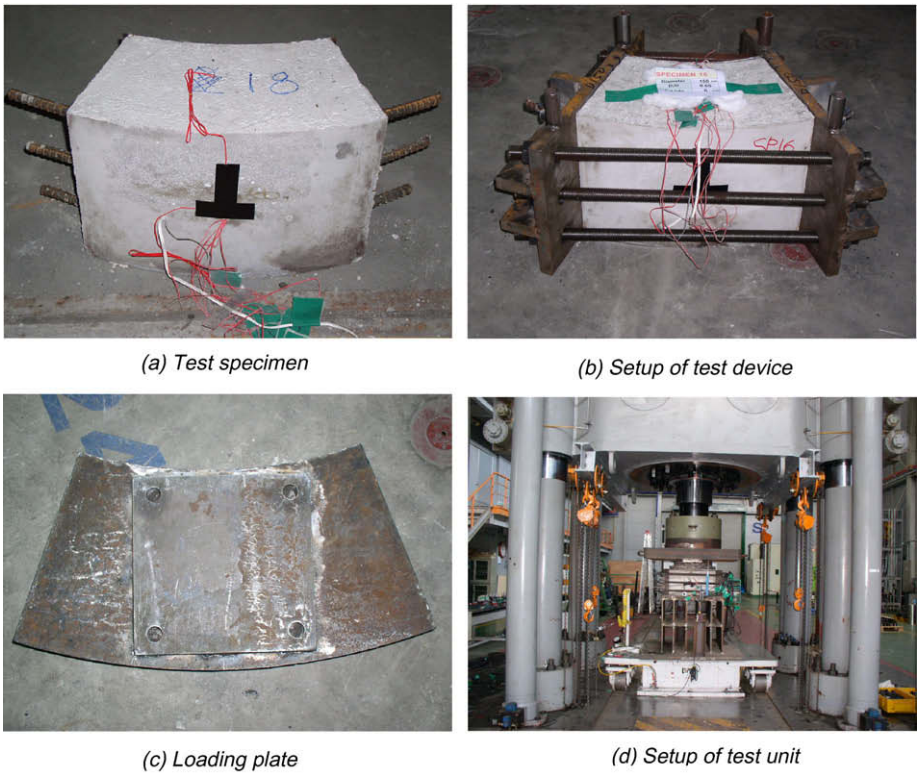

Fig. 11. Specimen and test device.

guidance in KSHB [22], and it was determined as 0.0075 for all specimens to have equal confining pressure in the circumferential direction. Table 3 shows the designed longitudinal and transverse reinforcements for the each specimen group. Figs. 8 and 9 show the designed specimens and their details.

4.2. Test unit and setup

For the test, some devices were designed and built to make equal boundary conditions to those of the real columns. Fig. 10 shows the designed test device. Fig. 11a and b shows the specimen and its installation into the test device. Two thick steel plates were placed at the both sides of the specimen and linked tightly with each other by steel rods. These steel plates restrain the circumferential displacements of the concrete by Poisson's effect during the test. They keep passive confining pressure to the specimen in the circumferential direction. To make the transverse reinforcements to exert the arching action, they were fabricated with initial curvatures and welded with the restraining steel plates. A curved steel plate was attached on the inner face of the specimen for the internal confinement. To apply axial load only on the concrete, corresponding loading plates were made for all specimens as shown in Fig. 11c. To minimize the deformation of the loading plate during the test, it was designed to have a minimum thickness of 100 mm. Fig. 11d shows the setup of the test unit.

The average compressive strength of the concrete was measured as 22.3 MPa from 28-day compression tests. The yield strength of the transverse and longitudinal reinforcements was 294 MPa from tests, and the yield strength of the curved steel plate was 253 MPa. Before the test, the expected failure modes of the specimens were predicted by Eqs. (12) and (16). Table 4 shows the calculated effective confining pressures and expected failure modes of the specimens. Because the specimens without the internal steel tube do not have confining pressure in the radial direction, they have the half effective confining pressure of the specimens with an internal tube. The required minimal thickness of the steel plate (internal tube) was described as t_{lim}.

Table 4
Confining pressure and expected failure mode.

Specimen	Effective confining pressure (kPa)	Yield stress of internal tube (kPa)	Buckling stress of internal tube (kPa)	t_{lim} (mm)	Failure mode
D150H65T0	514.2	–	–	–	–
D150H65T6	1028.4	253,000	5903.2	2.57	Mode 2
D150H75T0	514.2	–	–	–	–
D150H75T2	1028.4	253,000	492.7	2.97	Mode 1
D150H75T6	1028.4	253,000	4433.9	2.97	Mode 2
D200H65T2	1016.0	253,000	368.9	3.41	Mode 1
D200H65T4	1016.0	253,000	1475.8	3.41	Mode 2
D200H65T6	1016.0	253,000	3320.5	3.41	Mode 2
D200H70T0	508.0	–	–	–	–
D200H70T4	1016.0	253,000	1272.5	3.67	Mode 2
D200H70T6	1016.0	253,000	2863.1	3.67	Mode 2
D200H75T0	508.0	–	–	–	–
D200H75T2	1016.0	253,000	277.1	3.93	Mode 1
D200H75T6	1016.0	253,000	2494.1	3.93	Mode 2

Table 5
Test result.

Specimen	Strength (MPa)		Strength ratio (experiment/analysis) (%)
	Experiment	Analysis	
D150H65T0	26.532	24.971	106.2
D150H65T6	28.310	28.627	98.9
D150H75T0	23.331	26.155	89.2
D150H75T2	24.398	27.271	89.5
D150H75T6	29.689	28.627	103.7
D200H65T2	29.047	25.781	112.7
D200H65T4	30.606	28.642	106.9
D200H65T6	31.110	28.660	108.5
D200H70T0	22.880	25.349	90.3
D200H70T4	29.158	28.642	101.8
D200H70T6	29.026	28.660	101.3
D200H75T0	26.142	25.973	100.6
D200H75T2	29.401	27.063	108.6
D200H75T6	29.969	28.660	104.6

5. Test result

5.1. Strength enhancement

Test results show that the internal confinement exists and enhances the strength of the concrete. It means the internal confinement makes the concrete confined triaxially. The test group with an internal tube showed higher strength than the other group. Specimens which had been expected to show 'failure mode 2' showed higher strength than those had been expected to show 'failure mode 1'. Table 5 shows the test results and the analysis results by Eq. (2). In most cases, the experimental results were agreeable with the analysis results. Figs. 12 and 13 show the stress–strain relations from tests. All plots were offset to calibrate the initial displacements. In the test, applying a load was terminated before the transverse reinforcement yields because of the insufficient capacity of the loading machine. The test was finished when the applying load did not increase any more. Therefore, the ending strain in the plots does not mean the ductility of the specimen.

Fig. 12 shows the stress–strain relations of the specimens having the diameters (D) of 1500 mm. For D150H65 specimens in Fig. 12a, the minimal thicknesses of the internal tube to prevent its yielding and buckling failures were 2.086 mm and 2.571 mm, respectively. Therefore, the specimen D150H65T6 was expected to have 'failure mode 2'. For D150H75 specimens in Fig. 12b, the minimal thicknesses of the internal tube to prevent its yielding and buckling failures were 2.406 mm and 2.966 mm, respectively. The specimen D150H75T6 was expected to have 'failure mode 2'. The specimen D150H75T2 was expected to have 'failure mode 1' to show premature failure by buckling of the internal tube. The increased strengths by the internal confinement are summarized in

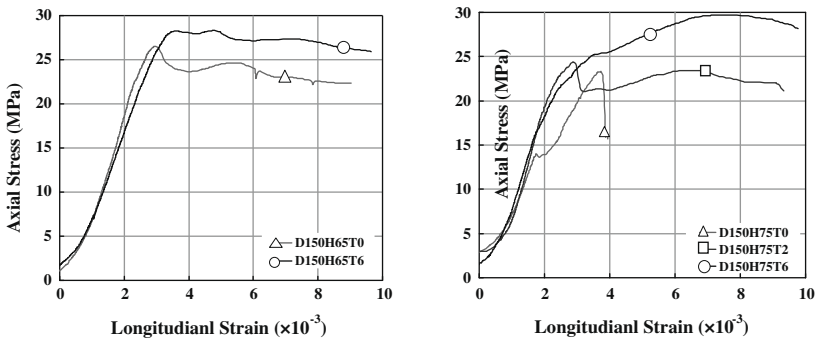

(a) hollow ratio=0.65 (b) hollow ratio=0.75

Fig. 12. Stress–strain relations of D150 Specimens.

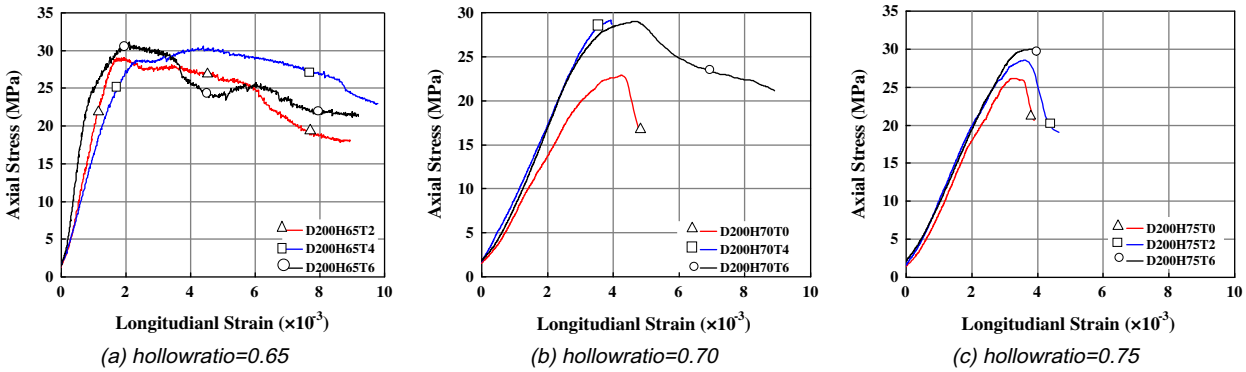

Fig. 13. Stress–strain relations of D200 Specimens.

Table 6
Increased strength.

Specimen	Strength (MPa)	Increased strength (MPa)	Increased strength ratio (%)	Failure mode
D150H65T0	26.532	4.232	19.0	–
D150H65T6	28.310	6.010	26.9	Mode 2
D150H75T0	23.331	1.031	4.6	
D150H75T2	24.398	2.098	9.4	Mode 1
D150H75T6	29.689	7.389	33.1	Mode 2
D200H65T2	29.047	6.747	30.3	Mode 1
D200H65T4	30.606	8.306	37.2	Mode 2
D200H65T6	31.110	8.810	39.5	Mode 2
D200H70T0	22.880	0.580	2.6	–
D200H70T4	29.158	6.858	30.8	Mode 2
D200H70T6	29.026	6.726	30.2	Mode 2
D200H75T0	26.142	3.842	17.2	–
D200H75T2	29.401	7.101	31.8	Mode 1
D200H75T6	29.969	7.669	34.4	Mode 2

Table 6, for all the specimens. It shows different amount of the increased strength by the internal confinement.

As the expectation, the specimens with an internal tube (D150H65T6, D150H75T2 and D150H75T6) showed higher strength than the others (D150H65T0 and D150H75T0). The specimens which were expected to have 'failure mode 2' showed the highest strength in their group. Although D150H75T0 and D150H75T2 specimens showed much smaller strength than the expectation, the test results showed agreeable strength and tendency with the analysis results as shown in Table 5.

Fig. 13 shows the stress–strain relations of the specimens having the diameters (D) of 2000 mm. For the D200H65 specimens in Fig. 13a, the minimal thicknesses of the internal tubes to prevent their yielding and buckling failures were 2.747 mm and 3.407 mm, respectively. Therefore, the D200H65T2 specimen was expected to show 'failure mode 1'. D200H65T4 and D200H65T6 specimens were expected to show 'failure mode 2', but all specimens seem to have shown 'failure mode 2' considering their plotting patterns. However, D200H65T4 and D200H65T6 specimens showed higher strength than D200H65T2 specimen as they had been estimated. The D200H65T2 specimen can be considered to have 'failure mode 1' by judging its lower strength than the others. All of them showed a little higher strength than the analysis result as shown in Table 5. The specimens having 'failure mode 2' (D200H65T4 and D200H65T6) showed almost equal strength to each other although the thicknesses of their internal tubes were different. Therefore, the thickness of the internal tube does not affect the concrete strength if it is larger than the required minimal thickness to prevent the premature failure of the ICH RC column.

In Fig. 13b and c, the stress–strain relations of the specimens having the internal tube (D200H70T4, D200H70T6 and D200H75T2, and D200H75T6) are compared with those of the specimens without the tube (D200H70T0 and D200H75T0). For the D200H70 specimens in Fig. 13b, the minimal thicknesses of the internal tubes to prevent their yielding and buckling failures were 2.959 mm and 3.667 mm, respectively. For the D200H75 specimens in Fig. 13c, the minimal thicknesses of the internal tubes to prevent their yielding and buckling failures were 3.170 mm and 3.931 mm, respectively. The specimens having the internal tube showed expected failure modes as shown in Table 4. Their strengths agreed with the analysis results as shown in Table 5. Because the D200H70T4 and D200H70T6 specimens had same failure mode (failure mode 2), they had almost equal concrete strength. Their concrete strengths were much larger than that of the specimen without an internal tube (D200H70T0). The specimen of D200H75T2 showed 'failure mode 1' as it had been expected. Fig. 14 shows its buckled steel plate (internal tube). Fig. 15 shows the inner faces of the specimens after the test. As shown in Fig. 15a, when a specimen had no internal tube to make the internal confinement (D200H70T0), the concrete on the inner face spalled out. When a specimen had an internal tube, the inner face did not spall owing to the internal confinement (D200H70T4) as shown Fig. 15b.

5.2. Failure modes and confined state

Fig. 16 shows the enhanced strengths and the average enhanced strengths of the specimens. Their average effective circumferential pressure was 1020.43 kPa. From the test, the average enhanced strength ratio was of 10.9% for the concrete in a hollow RC column

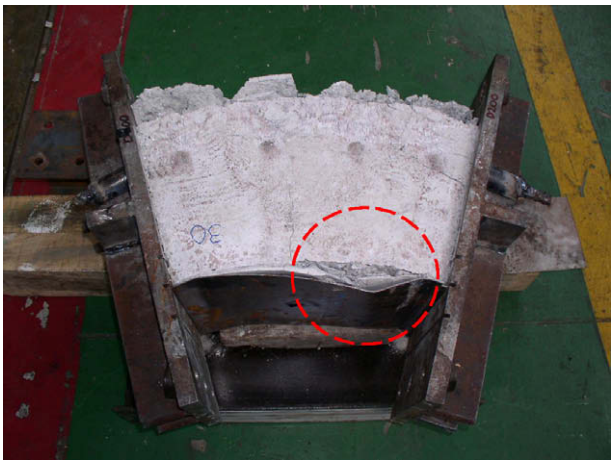

Fig. 14. Buckled steel plate of D200H75T2.

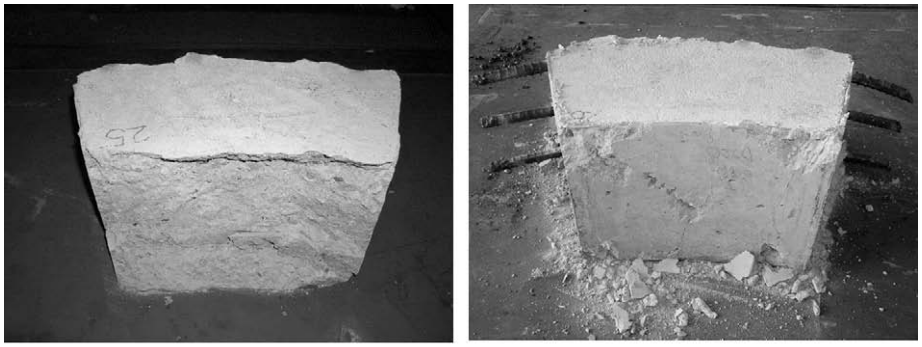

Fig. 15. Inner face of a specimen after test.

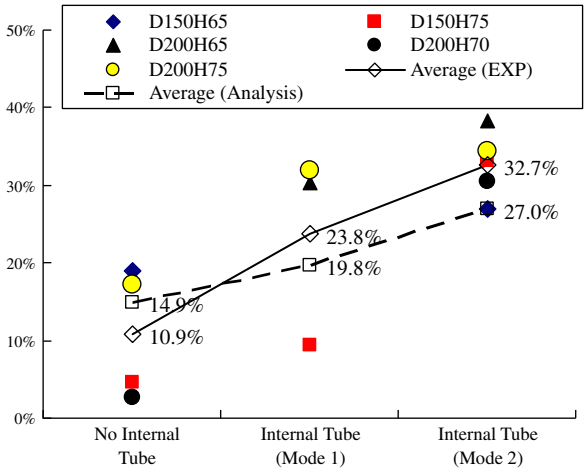

Fig. 16. Enhanced strength by internal confinement.

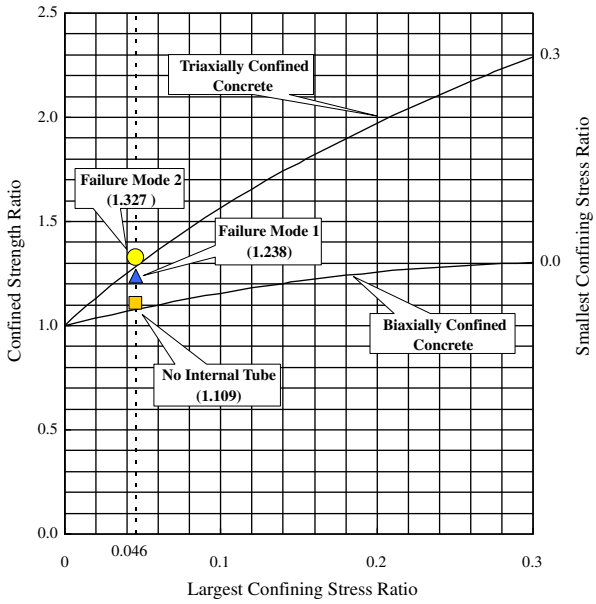

Fig. 17. Failure modes and confined state.

(t = 0, biaxially confined), when it was compared with the unconfined concrete strength (22.3 MPa). When an ICH RC column has 'failure mode 2', the enhanced concrete strength ratio was 32.7%. When an ICH RC column has 'failure mode 1', the enhanced concrete strength ratio was 23.8%. The test result showed higher strength than the analysis result for the concrete in ICH RC column specimens. From this result, it can be proved that the internal confinement exists, and it affects the strength of the concrete.

Fig. 17 shows the confined strength ratios as the failure modes. On the chart suggested by Mander et al. [11], the average confined strength ratios are dotted. From the average effective circumferential pressure (1020.43 kPa) and the unconfined concrete strength (22.3 MPa), the largest confining stress ratio was calculated as 0.046. Under this condition, the triaxially confined strength ratio was 1.327 from Eq. (2). The biaxially confined strength ratio was 1.109 from Eq. (7). The confined strength ratios from the test were 1.109, 1.238, and 1.327 for the specimens without an internal tube, the specimens having 'failure mode 1' and 'failure mode 2', respectively. As shown in Fig. 17, the specimen having 'failure mode 2' showed almost equal (3.14% higher) confined strength ratio to the triaxial confined state. This result means the existence of the internal confinement and it makes triaxial confinement. The specimen without an internal tube showed almost equal (2.82% higher) confined strength ratio to the biaxial confined state. This means the concrete is biaxially confined when the column has no internal tube. The gap of confined strength ratios between the triaxially confined state and the biaxially confined state is 0.208. The specimen having 'failure mode 1' had a 0.16 higher confined strength ratio than the specimen under the biaxial confined state. This amount is 77% of the gap (0.208) between triaxially confined state and biaxially confined state.

6. Conclusions

To show the existence of the internal confinement and to verify its effect on the concrete strength in an ICH RC column, an experiment was performed. Most test results agreed with the expected strengths and failure modes. They showed that the internal confinement prevented the spalling of the inner face of the concrete in an ICH RC column while the inner face of the concrete in a hollow RC column was spalled out. Therefore, the internal confinement enhances the strength of the concrete, and it can be offered by an internal tube. This internal confinement makes the concrete under triaxial confinement, and it was proved by the equal confined strength ratio of the concrete. It was shown that the defined possible failure modes of an ICH RC column were useful to estimate the concrete strength of an ICH RC column by the test results. They showed that the failure modes could be controlled by the thickness of the internal tube. Therefore, in designing an ICH RC column, the thickness of the internal tube is very important, and the internal

tube makes the concrete under triaxial confinement if it is thicker than the minimum requirement.

Acknowledgement

This work was supported by the Korea Research Foundation Grant funded by the Korean Government (MOEHRD). KRF-2007-357-D00245.

References

[1] Roy HEH, Sozen MA. Ductility of concrete. In: Proceedings of the international symposium on the flexural mechanics of reinforced concrete. ASCE-ACI; 1964. p. 213–24.
[2] Iyengar KTSR, Desayi P, Reddy TS. Stress–strain characteristics of concrete confined in steel binders. Mag Concr Res 1970;22(72):173–84.
[3] Desayi P, Iyengar KTSR, Reddy TS. Equations of stress–strain curve of concrete confined in circular steel spiral. Materiaux et Constructions 1978(September/October):339–45.
[4] Vallenas J, Bertero VV, Popov EP. Concrete confined by rectangular hoop subjected to axial loads. Report No. UCB/EERC-77/13. Berkeley: Earthquake Eng. Research Center, University of California; August 1977. p. 114.
[5] Sheikh SA, Uzumeri SM. Strength and ductility of tied concrete columns. ASCE 1980;106(ST5):1079–102.
[6] Scott BD, Park R, Priestley MJN. Stress–strain behavior of concrete confined by overlapping hoops at low and high strain rates. ACI J 1982(January–February):13–27.
[7] Sheikh SA, Uzumeri SM. Analytical model for concrete confinement in tied columns. J Struct Div ASCE 1982;108(12):2703–22.
[8] Sakino K, Sun YP. Stress–strain curve of concrete confined by rectilinear hoop. J Struct Constr Eng AIJ J 1984;461:95–104.
[9] Fafitis A, Shah SP. Predictions of ultimate behavior of confined columns subjected to large deformations. ACI J 1985(July–August):423–33.
[10] Chung HS, Yang KH, Lee YH, Eun HC. Stress–strain curve of laterally confined concrete. Eng Struct 2002;24:1153–63.
[11] Mander JB, Priestly MJN, Park R. Seismic design of bridge piers. Research Report No. 84-2. New Zealand: University of Canterbury; 1984
[12] Lin HJ, Liao CI, Yang C, Binici B. A numerical analysis of compressive strength of rectangular concrete columns confined by FRP. Comput Concr 2006;3(4):235–48.
[13] Lin HJ, Liao CI. Compressive strength of reinforced concrete column confined by composite material. Compos Struct 2004;65(2):239–50.
[14] Binici B. An analytical model for stress–strain behavior of confined concrete. Eng Struct 2005;27:1040–51.
[15] Mirmiran A, Shahawy M, Samaan M, El Echary H, Mastrapa JC, Pico O. Effect of column parameters on FRP-confined concrete. J Compos Constr 1998;2(4):175–85.
[16] Saafi M, Toutanji HA, Li Z. Behavior of concrete columns confined with fiber reinforced polymer tubes. ACI Mater J 1999;96(4):500–9.
[17] Han TH, Lim NH, Han SY, Park JS, Kang YJ. Nonlinear concrete model for an internally confined hollow reinforced concrete column. Mag Concr Res 2008;60(6):429–40.
[18] Popovics S. A numerical approach to the complete stress–strain curves of concrete. Cem Concr Res 1973;3(5):583–99.
[19] Kerr AD, Soifer MT. The linearization of the prebuckling state and its effects on the determined instability load. J Appl Mech 1969;36:775–85.
[20] Haftka RT, Mallet RH, Nachbar W. Adaptation of Koiter's method to finite element analysis of snap-through buckling behavior. Int J Solid Struct 1971;7:1427–45.
[21] Sun SM, Natori MC. Numerical solution of large deformation problems involving stability and unilateral constraints. Comput Struct 1996;58(6):1245–60.
[22] Korea Specification of Highway Bridge, Korean Ministry of Construction and Transportation; 2000.
[23] LUSAS manual (V13.4-6). FEA Ltd.; 2002.